

# A Trap Model for Clogging and Unclogging in Granular Hopper Flows

Alexandre Nicolas\*

*LPTMS, CNRS, Univ. Paris-Sud, Université Paris-Saclay, 91405 Orsay, France.*

Ángel Garcimartín and Iker Zuriguel

*Departamento de Física y Matemática Aplicada, Facultad de Ciencias, Universidad de Navarra, Pamplona, Spain*

(Dated: March 13, 2022)

Granular flows through narrow outlets may be interrupted by the formation of arches or vaults that clog the exit. These clogs may be destroyed by vibrations. A feature which remains elusive is the broad distribution  $p(\tau)$  of clog lifetimes  $\tau$  measured under constant vibrations. Here, we propose a simple model for arch-breaking, in which the vibrations are formally equivalent to thermal fluctuations in a Langevin equation; the rupture of an arch corresponds to the escape from an energy trap. We infer the distribution of trap depths from experiments and, using this distribution, we show that the model captures the empirically observed heavy tails in  $p(\tau)$ . These heavy tails flatten at large  $\tau$ , consistently with experimental observations under weak vibrations, but this flattening is found to be systematic, thus questioning the ability of gentle vibrations to restore a finite outflow forever. The trap model also replicates recent results on the effect of increasing gravity on the statistics of clog formation in a static silo. Therefore, the proposed framework points to a common physical underpinning to the processes of clogging and unclogging, despite their different statistics.

When discrete bodies flow through a constriction, there exists a risk of clogging, due to the spontaneous formation of arch-like (in two dimensions) or dome-like (in three dimensions) structures obstructing the bottleneck. This phenomenon can arise in an impressive variety of systems [1–5] and similar features have been observed in most of them, from granular packings flowing out of a vibrating silo [6] and colloids flowing through an orifice under a pressure gradient [7], to living beings, such as mice [8], sheep [9], and pedestrians [10]. In particular, while the flow intervals  $t_f$  between clogs are exponentially distributed, the distribution of lifetimes  $\tau$  of (temporary) individual clogs is heavy-tailed and can be fitted to a power law, viz.,  $p(\tau) \sim \tau^{-\alpha}$ . When the exponent  $\alpha$  is smaller than 2, the average clog lifetime  $\langle \tau \rangle$  does not converge; the mean outflow thus vanishes, which in practice means that extremely long clogs will dominate the process. This defines the clogged regime [9]. In contrast, a finite mean outflow is obtained for  $\alpha > 2$ , despite the flow intermittency.

In granular hopper flows, the unclogged regime  $\alpha > 2$  can be reached by enlarging the outlet or by applying stronger vibrations to the setup, both of which lead to larger values of  $\alpha$ , hence fewer long-lived clogs [9]. It is still debated whether clogs completely disappear above a critical outlet size in the absence of vibrations, or whether an (infinite) static silo will always clog up, *eventually* [11–14]. Beyond this conceptual question, differences have been put in the limelight between the static case and the shaken one. In particular, the formation of a clog and its destruction through vibrations follow different statistics, which has suggested that these processes are fundamentally distinct [6, 15–17]. Indeed, clogging is described as a Poissonian process characterized by a constant probability of formation of a stable arch. On the other hand,

the unclogging probability is not constant over time: The longer an arch has survived, the longer it will probably still live. Accordingly, this phenomenon was ascribed to aging [18], but so far this explanation has not been confirmed by experimental evidence.

In this Letter we promote a different explanation, centered on the heterogeneous *native* arch stabilities. We put forward a simple model that rationalizes the heavy tails of the unclogging process in vibrated silos. Remarkably, when applied to static silos, the model is found to reproduce several characteristic features, thus hinting at a common underpinning for clogging and unclogging.

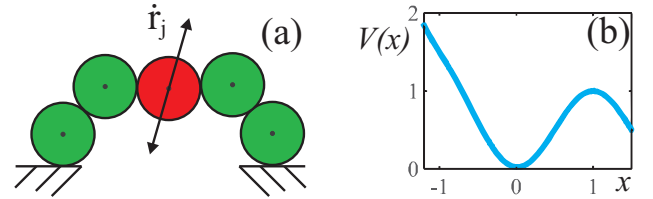


FIG. 1. (a) Sketch of an arch of vibrated grains. (b) Profile of the potential well used in the numerical simulations.

Consider the arch sketched in Fig. 1a, which is subjected to vertical vibrations characterized by a dimensionless acceleration  $\Gamma = \frac{A\omega^2}{g}$ , where  $A$  is the amplitude and  $\omega$  is the angular frequency. Newton’s equation of motion for grain  $j$  (at position  $\mathbf{r}_j$ ) reads

$$\ddot{\mathbf{r}}_j = -\frac{\partial V}{\partial \mathbf{r}_j}(\mathbf{r}_1, \dots, \mathbf{r}_N) + \mathbf{g} + \mathbf{f}_j + \xi(t)$$

where the mass of the grain has been set to one. The first term on the right-hand side accounts for the conservative interactions between grains ( $V$  is the global potential energy),  $\mathbf{g}$  is the gravity, and  $\mathbf{f}_j$  is a dissipative frictional

force. The vibrations induce an extra force  $\xi(t)$ . Let us focus on the weakest link  $j$  in the arch and overlook the deformation of the rest of the arch, whence we approximate  $V(\mathbf{r}_1, \dots, \mathbf{r}_N) \approx V(\mathbf{r}_j)$ . This is supported by experimental observations indicating that the particle with the largest angle dominates the breaking process [19]. To simplify the picture further, the gravitational potential energy is included in  $V$  and we assume quasi-one dimensional motion ( $\mathbf{r} \rightarrow x$ ), viz.,  $\ddot{x} = -V'(x) + f + \xi(t)$  where the  $j$  subscripts have been dropped. As vibrations are symmetric,  $\langle \xi(t) \rangle = 0$ . During the clogging event,  $\langle \ddot{x} \rangle \approx 0$  and  $V'(x)$  evolves much more slowly than  $\xi(t)$ , so taking the variance of the equation of motion over a small time window yields  $\langle \ddot{x}^2 \rangle \approx \langle \xi^2 \rangle$ . Here, we have also assumed that  $f$  increases at most linearly with the *velocity*  $|\dot{x}|$  of the grain, so that at high  $\omega$ ,  $\langle \ddot{x}^2 \rangle \sim \omega^2 \langle \dot{x}^2 \rangle \gg \langle f^2 \rangle$ . Finally, we note that the acceleration of the grain must be roughly proportional to the acceleration measured on the vibrated setup, viz.,  $\langle \ddot{x}^2 \rangle = \text{Tr}(\omega, \rho, \dots) \Gamma^2$ , where the transmission factor  $\text{Tr}$  includes the dependence on the material parameters of the grain, the frequency  $\omega$ , the density  $\rho$ , and so on. To leading order, overlooking these dependencies and the possible temporal correlations of the vibrations  $\xi(t)$ , we arrive at

$$\ddot{x} = -V'(x) + f + \xi(t) \quad (1)$$

with  $\langle \xi(t) \rangle = 0$  and  $\langle \xi(t) \xi(t') \rangle \propto \Gamma^2 \delta(t - t')$ . We notice that, in the case of viscous friction, i.e.,  $f \equiv -\gamma \dot{x}$  (with  $\gamma$  the drag coefficient), Eq. 1 is a Langevin equation with a vibration-induced Gaussian white noise associated with a temperature  $\beta^{-1} = \Gamma^2/\gamma$ . In the present work, we focus on this analytically tractable case, leaving for a separate study its generalization to other models of friction. The stability of the arch implies that  $x$  sits in a basin of  $V$ , constrained by an energy barrier of height, say,  $E_b$ . The hopping rate over such a barrier was worked out by Kramers [20] and reads

$$k \equiv \langle \tau \rangle^{-1} = \nu e^{-\beta E_b}, \quad (2)$$

where the attempt frequency  $\nu$  depends on  $\gamma$  and on the angular vibrational frequencies  $\omega_0$  and  $\omega_b$  at the minimum and at the saddle point. Kramers' formula holds in the moderate to high damping regime  $\gamma > \nu$ , for  $\beta E_b \ll 1$  (hence,  $k < \nu$ ). For a single  $E_b$ , hence a single  $k$ , different realizations of the noise yield an exponential distribution of escape times  $\tau$  [21]

$$p(\tau|k) = k e^{-k\tau} \quad (3)$$

In reality, energy barriers are expected to take a whole range of values, reflected by a distribution  $p(E_b)$ . So

will then the hopping rates  $k$ , by virtue of  $p(k)dk = p(E_b)dE_b$ . In this situation, the distribution of escape times  $\tau$  ( $\tau \geq \nu^{-1}$ ) is given by the convolution

$$p(\tau) = \int_0^\nu dk p(\tau|k) p(k). \quad (4)$$

The remaining step is to gather information on the features of the energy landscape, and more specifically  $p(E_b)$ . To do so, we exploit the arch-destabilization experiments performed by Lozano et al. [19], in which an acceleration ramp  $\Gamma(t) = \dot{\Gamma} t$  was applied to the arch until it breaks. An arch will typically break at an intensity  $\Gamma_c$  such that the breaking time  $\langle \tau \rangle$  is of the order of the experimental ramp time ( $\propto \dot{\Gamma}^{-1}$ ). Assimilating  $\tau$  to the escape time from a trap of depth  $E_b$  and using Eq. 2 with  $\beta = \frac{\gamma}{\Gamma^2}$ , we get  $E_b \approx \ln(\nu/\dot{\Gamma}) \Gamma_c^2/\gamma$ . Neglecting the weak (logarithmic) dependences on  $\nu$  and  $\dot{\Gamma}$ , we arrive at

$$E_b \approx \frac{\Gamma_c^2}{\gamma}. \quad (5)$$

More rigorous arguments [31] lead to the same scaling. Besides, it was observed that the average value  $\Gamma_c$  at which arches broke was virtually insensitive to  $\dot{\Gamma}$  in a given range [19]. Equation 5 implies that the exponential distributions  $p(\Gamma_c)$  measured experimentally for all tested outlet sizes  $D$  [23] translate into a Weibull distribution of energy barriers  $p(E_b)$ , viz.,

$$E_b = E_b^* y^a \text{ with } p(y) = e^{-y} \quad (6)$$

where  $a = 2$ ,  $y \equiv \frac{\Gamma_c}{\langle \Gamma_c \rangle}$  and  $E_b^*$  implicitly depends on  $D$ .

For more generality, we will nonetheless study Weibull distributions  $p(E_b)$  of arbitrary inverse shape parameters  $a$ . We start the discussion with the simple case  $a = 1$ , i.e., an exponential distribution. Equation 4 then turns into

$$p(\tau) = \epsilon \int_0^\nu dk e^{-k\tau} \left( \frac{k}{\nu} \right)^\epsilon,$$

where the dimensionless temperature  $\epsilon \equiv \frac{\Gamma_c^2}{\gamma E_b^*}$  has been introduced.

Changing variables to  $\tilde{k} \equiv k\tau$  and rescaling time as  $\tau \rightarrow \tilde{\tau} \equiv \nu\tau$ , one easily arrives at the pdf for  $\tilde{\tau}$ ,

$$p(\tilde{\tau}) = \frac{\epsilon}{\tilde{\tau}^{1+\epsilon}} \int_0^{\tilde{\tau}} d\tilde{k} e^{-\tilde{k}} \tilde{k}^\epsilon.$$

The complementary cumulative distribution function (CCDF)  $P(T > \tilde{\tau})$ , also called survival function, then reads

$$\begin{aligned} \int_{\tilde{\tau}}^\infty p(T) dT &= \epsilon \int_0^\infty dk e^{-k} k^\epsilon \int_{\max(k, \tilde{\tau})}^\infty dT T^{-1-\epsilon} \\ &= \left( \int_0^{\tilde{\tau}} dk e^{-k} k^\epsilon \right) \tilde{\tau}^{-\epsilon} + e^{-\tilde{\tau}} \approx \Gamma(1+\epsilon) \tilde{\tau}^{-\epsilon} \end{aligned} \quad (7)$$

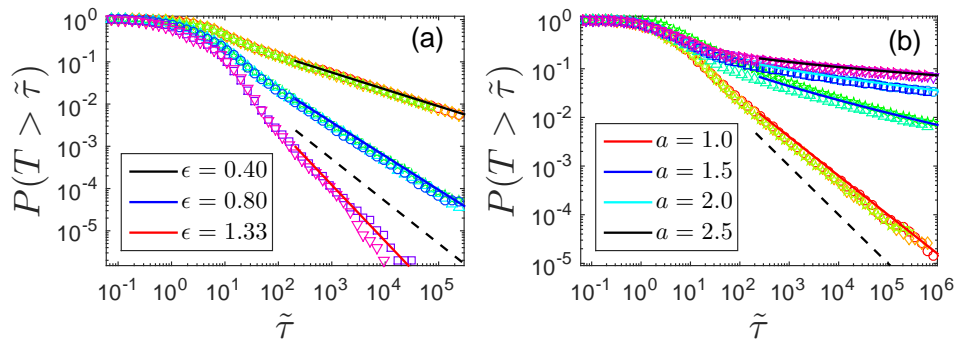


FIG. 2. **(a)** Survival functions  $P(T > \tilde{\tau})$  for an exponential distribution of barrier heights ( $a = 1$ ) as a function of rescaled time  $\tilde{\tau}$ , for the values of the vibrational temperature  $\epsilon$  indicated in the legend. **(b)** Survival functions  $P(T > \tilde{\tau})$  at fixed  $\epsilon = 0.8$ , for different shape parameters  $a$  versus  $\tilde{\tau}$ . In both plots, the different symbols refer to various parameter sets  $(\gamma, \Gamma, E_b^*)$ . The data collapse onto master curves coinciding with the predictions of Eqs. 7-8, shown as thick lines. The dashed lines in black have slope -1.

where we have introduced the Gamma function  $\Gamma$ , so

$$p(\tilde{\tau}) \approx \epsilon \Gamma(1 + \epsilon) \tilde{\tau}^{-1-\epsilon} \text{ for } \tilde{\tau} \rightarrow \infty.$$

The distribution of arch-breaking times thus follows a power law with exponent  $\alpha = 1 + \epsilon$  for  $\tilde{\tau} \rightarrow \infty$ . Therefore, the unclogging transition will be reached by simply increasing  $\epsilon$  (it takes place at  $\epsilon_c = 1$ ). Interestingly, the same power law tail distribution is obtained if a *single* escape time  $\tau$  is assigned to each energy barrier (hence, to each  $k$ ), instead of the distribution  $p(\tau|k)$  of Eq. 3. In this case, the description boils down to Bouchaud's trap model for aging in glasses [24], in which the system hops between exponentially distributed energy traps. Related models were also devised to explain e.g. the power-law blinking of semiconductor nanocrystals [25].

We test this result against numerical simulations relying on the velocity Verlet algorithm for stochastic dynamics [26]. To this end, a particular potential well has to be specified; we have chosen  $V(x) = \frac{E_b}{2}[1 - \cos(\pi x) + e^{-\pi(1+x)}]$  (see Fig. 1b) [32]. With this specific choice, the attempt frequency  $\nu$  is dependent on  $E_b$  (via  $\omega_0$  and  $\omega_b$ ). To account for this dependence, we invert Eq. 2 to get  $E_b(\tau) \approx E_b^* \epsilon \ln(\nu\tau)$ , where  $\nu$  is the attempt frequency for  $E_b = E_b^*$ , and we substitute  $\nu[E_b(\tau)]$  for  $\nu$  in the rescaled time  $\tilde{\tau} = \nu\tau$ . The validity of this approach is endorsed by the coincidence between the prediction of Eq. 7 and the simulation results (Fig. 2a).

A similar reasoning for the general case  $a > 0$  leads to an integral for the CCDF that cannot readily be expressed in closed form. Still, we can resort to the approximation indicated above, i.e., neglecting fluctuations for a given trap depth  $E_b$  and replacing  $p(\tau|k)$  with  $\delta(\tau - k^{-1})$ . The approximate CCDF can then be written as

$$P(T > \tilde{\tau}) \approx P[E_b(T) > E_b(\tilde{\tau})] \approx e^{-(\epsilon \ln \tilde{\tau})^{1/a}} \quad (8)$$

The numerical results obtained with the potential  $V(x)$  for different values of  $a$  (Fig. 2b) confirm the accuracy of this expression for long time lapses and thus support the validity of the approximation.

Let us now focus on the value  $a = 2$  which, as mentioned before, is the one that we inferred from the vibration ramp experiments. The CCDF  $P(T > \tau)$  for various vibrational temperatures  $\epsilon$  are plotted in Fig. 3a, as a function of non-rescaled time  $\tau$ . In the experimentally accessible region ( $P(T > \tau) > 10^{-3}$ ), delimited by the thick box on the figure, the survival functions are well described by power laws with exponents that hint at a transition between a clogged regime ( $\alpha \leq 2$ , diverging  $\langle \tau \rangle$ ) and an unclogged regime ( $\alpha > 2$ , converging  $\langle \tau \rangle$ ), in excellent agreement with experimental findings [33]. Experimentally, this transition was observed when increasing the vibration intensity  $\Gamma$  or the outlet size. Both changes come down to increasing  $\epsilon$  in the model, because  $\epsilon \sim \Gamma^2 / \langle \Gamma_c \rangle^2$  and the lower arch stabilities for larger outlets translate into lower typical energy barriers  $E_b^*$ , hence larger  $\epsilon$ . Quite interestingly, the model also captures the flattening of  $P(T > \tau)$  at large  $\tau$  that was observed experimentally for weak vibrations (especially at high frequencies) or narrow apertures [23], i.e., at small  $\epsilon$ . But, remarkably, the model suggests that this flattening is a *generic* property of gently shaken flows, which arises because of the heavier than exponential tail in  $p(E_b)$ .

The flattening of the survival function has crucial implications for the unclogging transition exposed above. Indeed, we notice from Eq. 8 that  $\langle \tau \rangle = \int_0^\infty P(T > \tau) d\tau$  diverges for any  $a > 1$ , regardless of the vibrational temperature  $\epsilon$ . Therefore, the model predicts that the system is always in the clogged regime, provided that the aperture gives rise to exponentially distributed arch stabilities  $\Gamma_c$  (Eq. 6 with  $a = 2$ ). The reasoning holds as long as (i) there is no upper cutoff in  $p(E_b)$  in the

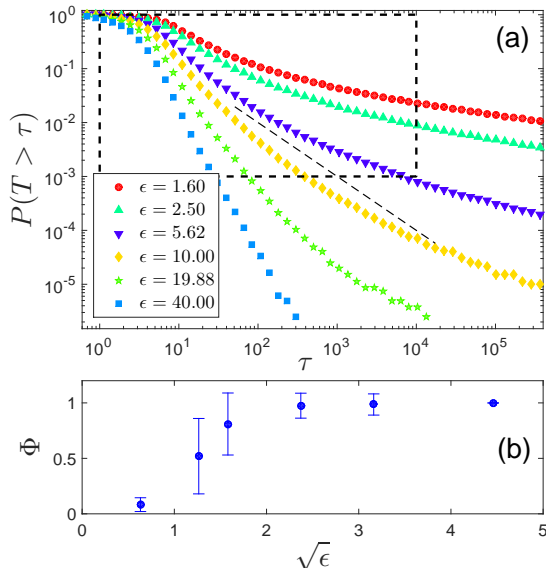


FIG. 3. (a) Survival functions  $P(T > \tau)$  as a function of dimensional time  $\tau$  for  $a = 2$ ,  $\gamma = 0.1$ ,  $E_b^* = 1$ , and different  $\epsilon$  as indicated in the legend. The box in thick dashed line indicates the experimentally accessible values. The thin dashed line has slope -1. (b) Duty cycle  $\Phi$  (see main text) calculated over a time window of 1000 s as a function of the vibrational acceleration  $\sqrt{\epsilon} \sim \Gamma$ , using the same parameters as in panel (a). For this calculation, the flow intervals were set to  $t_f = 10$  s and the model time unit was set to 1 ms, to get closer to the experimental values of [6]. The error bars represent standard deviations.

range of experimentally relevant values and (ii) vibrations are weak enough to not affect the granular density near the outlet, thus leaving  $p(E_b)$  mostly unaltered as compared to the vibrationless situation [17]. On no account does this conclusion prevent experiments of *finite* duration  $T$  from appearing to be in the flowing state if the vibrations are strong enough. Indeed, the duty cycle  $\Phi \equiv \langle t_f \rangle / (\langle t_f \rangle + \langle \tau \rangle)$ , which quantifies the fraction of time that the system spends effectively flowing, will reach finite values (intermittent flow) at high enough  $\epsilon$ , if it is computed within a temporal window of finite duration  $T$ . The example plotted in Fig. 3b for  $T = 1000$  s is in fact very similar to the measurements by Janda *et al.* (see Fig. 7 of [6], where  $1 - \Phi$  is plotted).

Now that several features of the unclogging process in vibrated silos have been recovered, let us extend the model to granular flows in static silos. When the system is flowing, the motion of grains creates an internal agitation, with a kinetic temperature proportional to the kinetic energy per grain:  $T_K \propto E_K$ . Using this temperature in our trap model, we expect the system to escape almost immediately from shallow traps  $E_b^{(j)} \leq E_K$ , where  $j = 1 \dots s - 1$  numbers the successive energy bar-

riers. Only when a barrier of height  $E_b^{(s)} > E_K$  is finally encountered will the system be arrested in the trap; without external agitation this halt will last forever. The clogging probability  $p_c$  per grain is then the probability to encounter such a high barrier,  $p_c = P(E_b > E_K)$ . Furthermore, under the assumption that the  $E_b^{(j)}$  are uncorrelated, the number  $s$  of grains that have escaped prior to clogging follows a Bernoulli process. This naturally leads to an exponential distribution of avalanches between clogs, with a mean size  $\langle s \rangle = p_c^{-1}$  for  $p_c \ll 1$ .

In a recent numerical work, Arevalo *et al.* computed the avalanche size for different values of gravity  $g_{\text{eff}}$  [29]. Besides confirming the expected scaling  $E_K \propto g_{\text{eff}}$  and showing that  $E_K$  is a prominent parameter for the description of the flow, their main result is the scaling law  $\ln \langle s \rangle \propto \sqrt{g_{\text{eff}}}$ . From these relations, we arrive at

$$P(E_b > E_K) = \exp\left(-b\sqrt{E_K}\right),$$

where  $b$  is a positive constant. Strikingly, the pdf derived from this CCDF takes the form

$$p(E_b) \sim \sqrt{\frac{E_b^*}{E_b}} \exp\left(-\sqrt{\frac{E_b}{E_b^*}}\right).$$

This is a Weibull distribution with exactly the same shape ( $a = 2$ ) as the one we inferred from ramp experiments in a vibrated silo. Thus, the distribution of energy barriers obtained in a vibrated silo is compatible with the avalanche size dependence on gravity in a static one.

In summary, we have put forward a model which likens unclogging at a bottleneck to the exploration of a simple energy landscape. We derived the statistics of escape times for a generic distribution of energy barriers. For the specific distribution inferred from measurements of arch stabilities, the escape time statistics are consistent with the heavy tails characteristic of flows through bottlenecks. An abundance of extremely long-lived clogs emerges generically in the model and it is thus suggested that gentle vibrations may not restore a permanent steady flow. The model is then extended to static silos, in which clogs persist forever if they can resist until the kinetic energy of all the grains is fully dissipated. We find that the variations of avalanche sizes with gravity reported recently stem from the very same distribution of barriers as that obtained from experiments in vibrated silos. This relation challenges the widespread idea that clogging and unclogging are independent processes that require separate interpretations.

AN is funded by Centre National de la Recherche Scientifique. AG and IZ acknowledge funding from Ministerio de Economía y Competitividad (Spanish Government) through Project No. FIS2014-57325 and FIS2017-84631. AN thanks Marie Chupeau for discussions.

### Determination of barrier heights from vibration ramp-up experiments

This section exposes the detail of calculations supporting our claim that, if stable arches (or vaults) are likened to energy traps which detain the system, the barrier height  $E_b$  can be determined from ramp experiments in which the vibrational intensity  $\Gamma$  is gradually increased from zero at a rate  $\dot{\Gamma}$  until the arch breaks, which occurs at a critical value  $\Gamma_c$ .

Let  $P_s(t) \in [0, 1]$  be the survival probability of an arch up to time  $t$ , with  $P_s(t=0) = 1$ . At a given vibrational intensity  $\Gamma = \dot{\Gamma}t$ , the arch-breaking rate is the Kramers escape rate  $\nu e^{-\beta E_b}$ , from Eq. 2 of the main text, so the survival probability evolves according to

$$-\dot{P}_s dt = P_s \nu e^{-\beta E_b} dt,$$

where  $P_s$  is the probability that the arch has survived so far and  $\beta = \gamma/(\dot{\Gamma}t)^2$ . Dividing both sides by  $P_s$  and integrating up to the breaking time  $t_c = \Gamma_c/\dot{\Gamma}$  yields

$$-\ln[P_s(t_c)] = \nu \int_0^{t_c} \exp\left(\frac{-\gamma E_b}{\dot{\Gamma}^2 t^2}\right) dt.$$

Since the arch will typically break when its survival probability is  $1/2$ , after a change of integration variables from  $t$  to  $u = \dot{\Gamma}t/\sqrt{\gamma E_b}$ , one arrives at

$$\begin{aligned} \ln(2) &= \frac{\nu \sqrt{\gamma E_b}}{\dot{\Gamma}} F\left(\frac{\dot{\Gamma} t_c}{\sqrt{\gamma E_b}}\right), \\ \frac{\dot{\Gamma} \ln(2)}{\nu \sqrt{\gamma E_b}} &= F\left(\frac{\Gamma_c}{\sqrt{\gamma E_b}}\right) \end{aligned} \quad (\text{S1})$$

with  $F(x) = \int_0^x \exp(-u^{-2}) du$ . At first sight, solving Eq. S1 for  $E_b$  looks challenging. However, it suffices to notice that the monotonic function  $F(x)$  sharply increases from  $10^{-7}$  to  $5 \cdot 10^{-3}$  when  $x$  spans the (narrow) range  $[0.3, 0.6]$ . Experimentally, the ratio  $\frac{\dot{\Gamma} \ln(2)}{\nu \sqrt{\gamma E_b}}$  appearing in Eq. S1 most probably took values around  $10^{-5}$  in [19, 23, 30]. Indeed,  $\sqrt{\gamma E_b} \sim \Gamma_c$  (very roughly speaking, from the leading order of Eq. S1),  $\dot{\Gamma}/\Gamma_c \approx 10^{-2}$ , and it is sensible to approximate the attempt frequency  $\nu$  with the vibration frequency, of order  $10^2 - 10^3$  Hz (see *e.g.* Table II of [23]), for want of a more accurate value. Therefore, the argument  $(\Gamma_c/\sqrt{\gamma E_b})$  of  $F$  is between 0.3 and 0.6 (and very probably between 0.35 and 0.5), so

$$\gamma E_b \approx 6\Gamma_c^2 \pm 2\Gamma_c^2. \quad (\text{S2})$$

We have thus shown how to relate the barrier height  $E_b$  to the critical vibrational intensity  $\Gamma_c$ .

### Comparison of the distribution of clog durations with experimental data

This section is aimed at providing a direct comparison between the distributions of clog durations  $\tau$  found

with our trap model and experimental ones. To this end, we consider Lozano et al.'s two-dimensional hopper flow experiments for an aperture of width  $D = 4.2$  particle diameters, in the presence of vibrations of frequency 1 kHz. For this frequency, critical vibration intensities  $\Gamma_c$  (see the previous section) were measured in ramp-up experiments for apertures  $D \in [3.2, 4.5]$ . From these measurements, shown in Fig. 3.11 (p. 72) of [30], we can interpolate that  $\langle \Gamma_c \rangle \simeq 1.7$  for  $D = 4.2$ .

The vibrational intensities  $\Gamma = 3.5, 4.0, 5.0$ , and  $7.0$  studied experimentally then correspond to vibrational temperatures  $\epsilon = 1.0, 1.4, 2.1$ , and  $4.2$ . To obtain these correspondences, we have made use of  $E_b \approx 4\Gamma_c^2/\gamma$  (where we arbitrarily chose the lower bound in Eq. S2, because it gives better results) and  $E_b = E_b^* \Gamma_c^2 / \langle \Gamma_c \rangle^2$  (Eq. 5 of the main text), hence  $\gamma E_b^* \approx 4 \langle \Gamma_c \rangle^2$  and  $\epsilon \equiv \frac{\Gamma^2}{\gamma E_b^*} = \frac{1}{4} \frac{\Gamma^2}{\langle \Gamma_c \rangle^2}$ . The survival functions (CCDF)  $P(T > \tau)$  of clog durations  $\tau$  found in the model are directly compared to the experimental ones in Fig. S1. Given the simplicity of our trap model and bearing in mind that the main trends of the CCDF only depend on one parameter,  $\epsilon$ , the agreement is deemed quite satisfactory, albeit imperfect.

Varying the setup, we now consider an aperture of width  $D = 4.76$  with vibrations of frequency 100 Hz. Unfortunately, ramp experiments were not performed experimentally in this setup to measure  $\Gamma_c$ . All we can do is to assume that, for this aperture, the ratio of the mean critical values  $\langle \Gamma_c \rangle$  for vibration frequencies 100Hz and 1000Hz is similar to that measured for an aperture  $D = 4.0$ , i.e.,  $\frac{0.40}{1.80} \simeq 0.22$ , following Table I of [23]. Then, we expect  $\langle \Gamma_c \rangle = 0.31$  at a frequency of 100Hz for  $D = 4.76$ . It follows that vibrational intensities  $\Gamma = 1.0, 1.5, 2.0$ , and  $2.6$  correspond to  $\epsilon = 2.6, 5.9, 10.5$ , and  $17.8$ . Figure S2 presents the comparison between the experimental CCDF and the modeled CCDF. Once again, we find satisfactory agreement.

---

\* alexandre.nicolas@polytechnique.edu

- [1] D. Helbing, I. Farkas, and T. Vicsek, "Simulating dynamical features of escape panic," *Nature*, vol. 407, no. 6803, pp. 487–491, 2000.
- [2] K. To, P.-Y. Lai, and H. K. Pak, "Jamming of granular flow in a two-dimensional hopper," *Physical Review Letters*, vol. 86, no. 1, p. 71, 2001.
- [3] M. Delarue, J. Hartung, C. Schreck, P. Gniewek, L. Hu, S. Herminghaus, and O. Hallatschek, "Self-driven jamming in growing microbial populations," *Nature physics*, vol. 12, no. 8, p. 762, 2016.
- [4] M. Haw, "Jamming, two-fluid behavior, and self-filtration in concentrated particulate suspensions," *Physical Review Letters*, vol. 92, no. 18, p. 185506, 2004.
- [5] D. Genovese and J. Sprakel, "Crystallization and intermittent dynamics in constricted microfluidic flows of



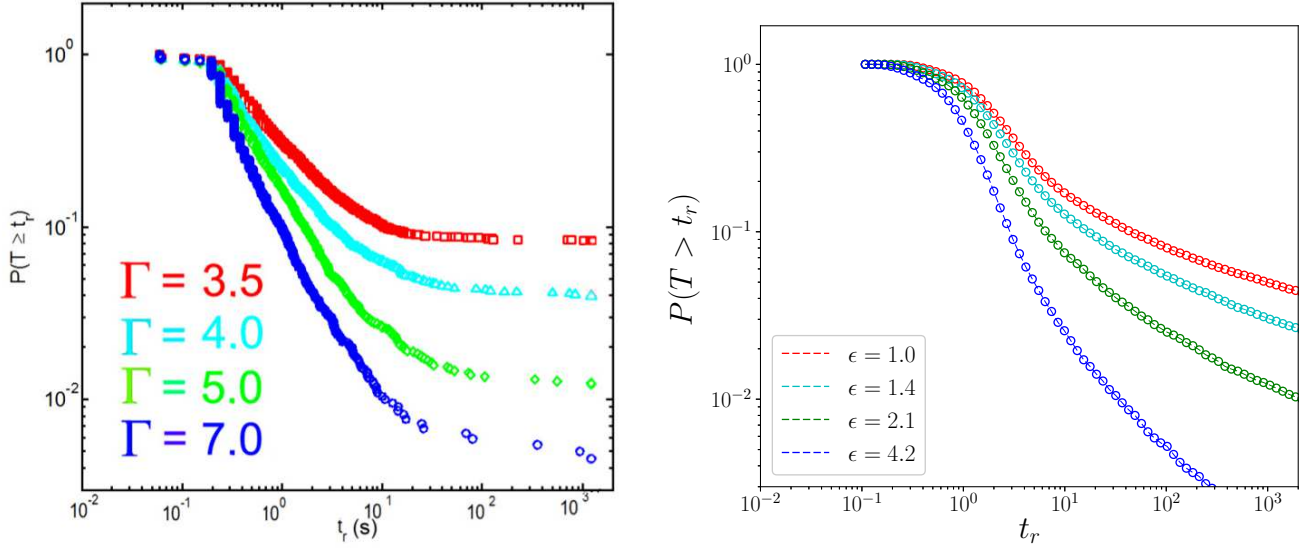


FIG. S1. Survival function  $P(T \geq t_r)$  of clog durations  $t_r$  (called  $\tau$  in the main text) in Lozano's two-dimensional experiments at a vibration frequency of 1 kHz and for an aperture of width  $D = 4.2$  (left) and in our trap model, with  $\gamma = 0.3$  and  $E_b^* = 1$  (right). The left panel was taken from [30] (p. 101). The model time unit was set to 0.2 s to facilitate the comparison. Notice that both panels are plotted with identical axes.

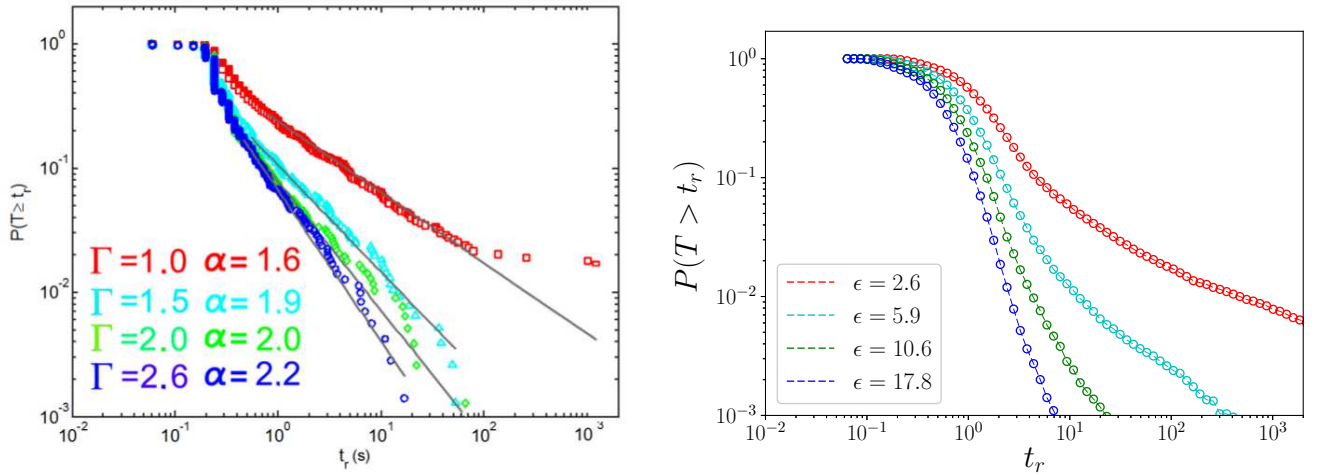


FIG. S2. Survival function  $P(T \geq t_r)$  of clog durations  $t_r$  measured experimentally at a frequency of 100 Hz and for an aperture  $D = 4.76$  (left) and in our trap model, with parameters  $(\gamma, E_b^*)$  identical to Fig. S1 (right). The left panel was taken from [30] (Fig. 3.28, p. 94). The model time unit was set to 0.2 s.

- dense suspensions," *Soft Matter*, vol. 7, no. 8, pp. 3889–3896, 2011.
- [6] A. Janda, D. Maza, A. Garcimartín, E. Kolb, J. Lanuza, and E. Clément, "Unjamming a granular hopper by vibration," *EPL (Europhysics Letters)*, vol. 87, no. 2, p. 24002, 2009.
- [7] R. C. Hidalgo, A. Goñi Arana, A. Hernández-Puerta, and I. Pagonabarraga, "Flow of colloidal suspensions through small orifices," *Physical Review E*, vol. 97, p. 012611, 2018.
- [8] P. Lin, J. Ma, T. Liu, T. Ran, Y. Si, and T. Li, "An experimental study of the "faster-is-slower" effect using mice under panic," *Physica A: Statistical Mechanics and its Applications*, vol. 452, pp. 157–166, 2016.
- [9] I. Zuriguel, D. R. Parisi, R. C. Hidalgo, C. Lozano, A. Janda, P. A. Gago, J. P. Peralta, L. M. Ferrer, L. A. Pugnaloni, E. Clément, *et al.*, "Clogging transition of many-particle systems flowing through bottlenecks," *Scientific Reports*, vol. 4, p. 7324, 2014.
- [10] J. M. Pastor, A. Garcimartín, P. A. Gago, J. P. Peralta, C. Martín-Gómez, L. M. Ferrer, D. Maza, D. R. Parisi, L. A. Pugnaloni, and I. Zuriguel, "Experimental proof of faster-is-slower in systems of frictional particles flowing through constrictions," *Physical Review E*, vol. 92, no. 6, p. 062817, 2015.
- [11] I. Zuriguel, A. Garcimartín, D. Maza, L. A. Pugnaloni,

- and J. M. Pastor, “Jamming during the discharge of granular matter from a silo,” *Physical Review E*, vol. 71, no. 5, p. 051303, 2005.
- [12] K. To, “Jamming transition in two-dimensional hoppers and silos,” *Physical Review E*, vol. 71, no. 6, p. 060301, 2005.
- [13] C. C. Thomas and D. J. Durian, “Geometry dependence of the clogging transition in tilted hoppers,” *Physical Review E*, vol. 87, no. 5, p. 052201, 2013.
- [14] C. C. Thomas and D. J. Durian, “Fraction of clogging configurations sampled by granular hopper flow,” *Physical Review Letters*, vol. 114, no. 17, p. 178001, 2015.
- [15] K. To and H.-T. Tai, “Flow and clog in a silo with oscillating exit,” *Phys. Rev. E*, vol. 96, p. 032906, Sep 2017.
- [16] I. Zuriguel, Á. Janda, R. Arévalo, D. Maza, and Á. Garcimartín, “Clogging and unclogging of many-particle systems passing through a bottleneck,” in *EPJ Web of Conferences*, vol. 140, p. 01002, EDP Sciences, 2017.
- [17] C. Mankoc, A. Garcimartín, I. Zuriguel, D. Maza, and L. A. Pugnaloni, “Role of vibrations in the jamming and unjamming of grains discharging from a silo,” *Physical Review E*, vol. 80, no. 1, p. 011309, 2009.
- [18] B. Blanc, J.-C. Géminard, and L. Pugnaloni, “On-and-off dynamics of a creeping frictional system,” *the European Physical Journal E*, vol. 37, p. 112, 2014.
- [19] C. Lozano, G. Lumay, I. Zuriguel, R. C. Hidalgo, and A. Garcimartín, “Breaking arches with vibrations: the role of defects,” *Physical Review Letters*, vol. 109, no. 6, p. 068001, 2012.
- [20] H. Kramers, “Brownian motion in a field of force and the diffusion model of chemical reactions,” *Physica*, vol. 7, no. 4, pp. 284–304, 1940.
- [21] P. Hänggi, P. Talkner, and M. Borkovec, “Reaction-rate theory: fifty years after kramers,” *Reviews of modern physics*, vol. 62, no. 2, p. 251, 1990.
- [22] These arguments are exposed in the Supplemental Material.
- [23] C. Lozano, I. Zuriguel, and A. Garcimartín, “Stability of clogging arches in a silo submitted to vertical vibrations,” *Physical Review E*, vol. 91, no. 6, p. 062203, 2015.
- [24] J.-P. Bouchaud, “Weak ergodicity breaking and aging in disordered systems,” *Journal de Physique I*, vol. 2, no. 9, pp. 1705–1713, 1992.
- [25] R. Verberk, A. M. van Oijen, and M. Orrit, “Simple model for the power-law blinking of single semiconductor nanocrystals,” *Physical Review B*, vol. 66, no. 23, p. 233202, 2002.
- [26] N. Grønbech-Jensen and O. Farago, “A simple and effective verlet-type algorithm for simulating langevin dynamics,” *Molecular Physics*, vol. 111, no. 8, pp. 983–991, 2013.
- [27] Another potential function,  $V(x) = \frac{E_b}{8}[(1 - \cos(\pi x))^3 + 4e^{-\pi(1+x)}]$ , was tested and was found to yield almost identical results.
- [28] A more direct comparison with experimental data is proposed in the Supplemental Material.
- [29] R. Arévalo and I. Zuriguel, “Clogging of granular materials in silos: effect of gravity and outlet size,” *Soft Matter*, vol. 12, no. 1, pp. 123–130, 2016.
- [30] C. Lozano, *Estabilidad de los arcos de un medio granular frente a vibraciones*. PhD thesis, Universidad de Navarra, 2014.
- [31] These arguments are exposed in the Supplemental Material.
- [32] Another potential function,  $V(x) = \frac{E_b}{8}[(1 - \cos(\pi x))^3 + 4e^{-\pi(1+x)}]$ , was tested and was found to yield almost identical results.
- [33] A more direct comparison with experimental data is proposed in the Supplemental Material